IV. WISE Data Processing

4. Pipeline Science Modules

h. Photometric Calibration

Contents

i. Summary and Useful Formulas

All magnitudes listed in the WISE Source Catalog and Single-Exposure Source Database have been photometrically calibrated using observations of a network of standard stars that are located near the ecliptic polar caps, as described in IV.4.h.ii. For WISE Atlas and Single-exposure Images, photometric zero points that allow direct conversion of pixel intensity values to calibrated magnitudes, are derived for calibrators throughout the WISE mission. The photometric zero point values are provided in the MAGZP keyword values in the FITS image headers.

This section on Photometric Calibration describes in more detail the process by which instrumental source magnitudes were converted to calibrated magnitudes, and how the photometric zero point levels were derived for WISE. A brief introduction to the WISE photometric system is given below. Additional information can be found in Wright et al. (2010 AJ, 140, 1868) and Jarrett et al. (2011 ApJ, 735, 112).

All reported magnitudes are in the Vega System. Formulae for converting WISE Vega magnitudes to flux density units (in Janskys) and AB magnitudes are given below along with two practical examples.

1. Vega Magnitudes to Flux Density

The source flux density, in Jansky [Jy] units, is computed from the calibrated WISE magnitudes, m_{vega} using:

$$F_\nu[Jy] = F_{\nu 0} \times 10^{(-m_{vega}/2.5)} \quad \text{(Eq. 1)}$$

where $F_{\nu 0}$ is the zero magnitude flux density corresponding to the constant that gives the same response as that of Alpha Lyrae (Vega). *For most sources, the zero magnitude flux density, derived using a constant power-law spectra, is appropriate and may be used to convert WISE magnitudes to flux density [Jy] units*. Table 1 lists the zero magnitude flux density (column 2) for each WISE band.

For sources with steeply rising MIR spectra or with spectra that deviate significantly from F_ν=constant, including cool asteroids and dusty star-forming galaxies, a color correction is required, especially for W3 due to its wide bandpass. With a given flux correction, f_c, the flux density conversion is given by:

$$F_\nu[Jy] = (F^*_{\nu 0}/f_c) \times 10^{(-m_{vega}/2.5)} \quad \text{(Eq. 2)}$$

where $F^*_{\nu 0}$ is the zero magnitude flux density derived for sources with power-law spectra: $F_\nu \propto \nu^{-2}$, listed in Table 1 (column 3) and the flux correction, f_c, listed in Table 2 for $F_\nu \propto \nu^{-\alpha}$, where the index α ranges from: -3, -2, -1, 0, 1, 2, 3, and 4, and for blackbody spectra, $B_\nu(T)$ for a variety of temperatures, and for stars of two main-sequence spectral types (K2V and G2V).

Table 1- Zero Magnitude Flux Density

Band	$F_{\nu 0}$ [Jy]	$F^*_{\nu 0}$ [Jy]
W1	309.540	306.682
W2	171.787	170.663
W3	31.674	29.045
W4	8.363	8.284

where $F_{\nu 0}$ is the flux density for sources with constant power-law spectra: $F_\nu \propto \nu^0$; in the third column, $F^*_{\nu 0}$ is the flux density for sources with power-law spectra: $F_\nu \propto \nu^{-2}$, and is used for color corrections such that $F_{\nu 0} = F^*_{\nu 0} / f_c$, where fc is the flux correction given in Table 2.

Table 2- Color corrections (from Wright et al. 2010)

FLUX CORRECTIONS AND COLORS FOR POWERLAWS AND BLACKBODIES

F_ν	$f_c(W1)$	$f_c(W2)$	$f_c(W3)$	$f_c(W4)$	[W1-W2]	[W2-W3]	[W3-W4]
ν^3	1.0283	1.0206	1.1344	1.0142	-0.4040	-0.9624	-0.8684
ν^2	1.0084	1.0066	1.0088	1.0013	-0.0538	-0.0748	-0.0519
ν^1	0.9961	0.9976	0.9393	0.9934	0.2939	0.8575	0.7200
ν^0	0.9907	0.9935	0.9169	0.9905	0.6393	1.8357	1.4458
ν^{-1}	0.9921	0.9943	0.9373	0.9926	0.9828	2.8586	2.1272
ν^{-2}	1.0000	1.0000	1.0000	1.0000	1.3246	3.9225	2.7680
ν^{-3}	1.0142	1.0107	1.1081	1.0130	1.6649	5.0223	3.3734
ν^{-4}	1.0347	1.0265	1.2687	1.0319	2.0041	6.1524	3.9495
$B_\nu(100)$	17.2062	3.9096	2.6588	1.0032	10.6511	18.9307	4.6367
$B_\nu(141)$	4.0882	1.9739	1.4002	0.9852	7.7894	13.0371	3.4496
$B_\nu(200)$	2.0577	1.3448	1.0006	0.9833	5.4702	8.8172	2.4949
$B_\nu(283)$	1.3917	1.1124	0.8791	0.9865	3.8329	5.8986	1.7552
$B_\nu(400)$	1.1316	1.0229	0.8622	0.9903	2.6588	3.8930	1.2014
$B_\nu(566)$	1.0263	0.9919	0.8833	0.9935	1.8069	2.5293	0.8041
$B_\nu(800)$	0.9884	0.9853	0.9125	0.9958	1.1996	1.6282	0.5311
$B_\nu(1131)$	0.9801	0.9877	0.9386	0.9975	0.7774	1.0421	0.3463
K2V	1.0038	1.0512	1.0030	1.0013	-0.0963	0.1225	-0.0201
G2V	1.0049	1.0193	1.0024	1.0012	-0.0268	0.0397	-0.0217

2. Additional W4 Correction for "Red" Sources

Because of uncertainty in the calibration of the W4 Relative Spectral Response (RSR), sources that have a steeply rising mid-IR spectrum, $F_\nu \propto \nu^{-\alpha}$ where α >= 1, require approximately an 8 to 10% correction to the W4 flux, as follows:

$$F_\nu^{'}[W4] \approx 0.90 \times F_\nu[\mathrm{W4}], \;\; \text{when } \mathrm{F}_\nu \propto \nu^{-(\alpha > 1)} \quad \text{(Eq. 3)}$$

Additional details are given in Discrepancy between blue and red source measurements.

3. Vega to AB Magnitudes

Monochromatic AB magnitudes are defined by $-2.5\log(F_\nu[Jy]) + 8.926$ (see e.g., Tokunaga & Vaca 2005). Hence, conversion from the WISE Vega-system magnitudes to flux density using $F_{\nu 0}$ (column 2 of Table 1) and to AB magnitudes follows:

$$m_{ab} = m_{vega} + \Delta m \quad \text{(Eq. 4)}$$

where Δm is the constant magnitude offset specified in Table 3.

Table 3 - Conversion to the AB system ($m_{AB} = m_{Vega} + \Delta m$)

Band	magnitude offset (Δm)
W1	2.699
W2	3.339
W3	5.174
W4	6.620

4. Examples for Converting WISE Magnitudes to Flux Densities

Case 1 (blue source) -- WISE J091538.49+095230

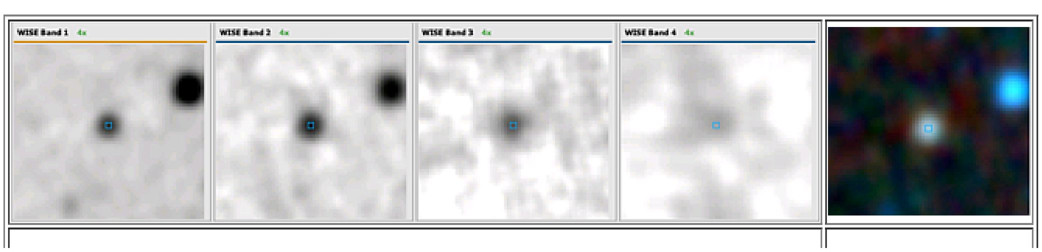

Figure 1a - WISE W1, W2, W3 and W4 Atlas Images of source J091538.49+095230. The field of view is 90 arcsec.	**Figure 1b -** 3-color composite image: blue = W1, green = W2, red = W3.

WISE J091538.49+095230 is a QSO at z= 0.62 (SDSS J091538.48+095230.0), a relatively "blue" extragalactic object that is well detected in the first three WISE bands and detected, but quite faint (SNR ~ 4) in W4. The profile-fit magnitudes (w?mpro) in the All-Sky Release Catalog for this sources are listed in column 2 of Table 4.

Table 4 - Photometry of WISE J091538.49+095230 using Eq. 2

band	**w?mpro (unc)**	**F_ν(corr) (unc)**
	mag	mJy
W1	14.474 (0.035)	0.50 (0.02)
W2	13.318 (0.037)	0.81 (0.03)
W3	10.465 (0.082)	2.02 (0.15)
W4	8.059 (0.245)	4.99 (1.13)

The colors of this source are: [W1-W2] = 1.16 mag and [W2-W3] = 2.85 mag. Looking at the spectral colors in Table 2, the source appears to have spectral slope that is somewhat flat, an index between "0" and "1" for $F_\nu \propto \nu^{-\alpha}$. For a slope of "1", the corresponding flux corrections are: 0.992, 0.994, 0.937, 0.993, applied with $F_{\nu 0} = F^*_{\nu 0} / f_c$. The corrected, monochromatic (λ_{iso}) flux densities after application of the flux corrections are listed in column 3 of Table 4

Finally, as noted above, most stars and galaxies (with $\alpha < 1$) do not require a color correction. Simply using the constant power-law conversion, $F_{\nu 0}$ (column 2 of Table 1) provides a reasonable conversion to flux density. The monochromatic flux densities using the constant power-law conversion are listed in Table 5, and are nearly identical to the color-corrected versions shown in Table 4.

Table 5 - Photometry of WISE J091538.49+095230 using Eq. 1

band	w?mpro (unc)	F_ν(corr) (unc)
	mag	mJy
W1	14.474 (0.035)	0.50 (0.02)
W2	13.318 (0.037)	0.81 (0.03)
W3	10.465 (0.082)	2.06 (0.15)
W4	8.059 (0.245)	5.00 (1.13)

Case 2 (red source) -- WISE J145606.01+193839.6

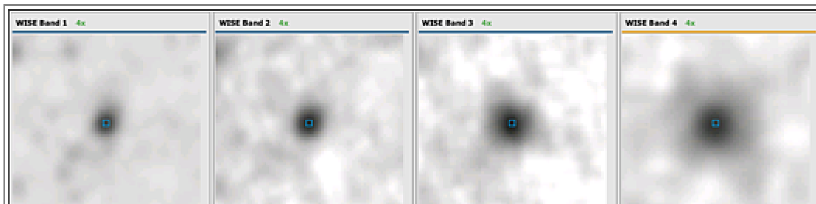

Figure 2a - WISE W1, W2, W3 and W4 Atlas Images of source J145606.01+193839.6. The field of view is 90 arcsec.

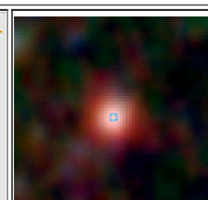

Figure 2b - 3-color composite image: blue = W1, green = W2, red = W3.

This strikingly red WISE source is associated with the IRAS source IRAS F14537+1950 (z = 0.64), a starbursting hyperluminous infrared galaxy. The WISE All-Sky Release Catalog photometry for this source is given in column 2 of Table 6, below.

Table 6 - Photometry of WISE source J145606.01+193839.6 using Eq. 2

band	w?mpro (unc)	F_ν(corr) (unc)
	mag	mJy
W1	14.492 (0.029)	0.49 (0.01)

W2	14.012 (0.037)	0.42 (0.01)
W3	9.985 (0.038)	2.94 (0.10)
W4	6.656 (0.056)	16.58 (0.86)

The colors of this source are: [W1-W2] = 0.48 mag and [W2-W3] = 4.03 mag. Looking at the spectral colors in Table 2, the source appears to have an index between "2" and "3" for $F_\nu \propto \nu^{-\alpha}$. The corresponding flux corrections (adopting an index of 2) are unity for all bands, as used with $F_{\nu 0} = F^*_{\nu 0} / f_c$. This source has a rising mid-IR color (α > 1), and thus W4 needs an additional 8% correction to its flux (that is, decrease the flux by 8%) to account for the blue vs. red calibration discrepancy. Applying the flux corrections and $F^*_{\nu 0}$, and the W4 8% correction (Eq. 3) gives the monochromatic (λ_{iso}) flux densities given in column 3 of Table 6.

Note that adopting the flat-spectrum constant $F_{\nu 0}$ (Eq. 1) gives a slightly larger W3 flux of 3.21 mJy. The reason for this is that more of the galaxy light comes from the long-wavelength side of the W3 RSR. To get the calibrated flux corresponding to the light that is centered near the W3 λ(iso), an appropriate correction (Eq. 2) is needed to adjust for source spectral shape convolved with the WISE RSR shape.

ii. WISE Calibration Source Network

WISE is calibrated on the same absolute basis as that established for the Spitzer Space Telescope. Networks of calibration stars support Spitzer observations with IRAC, MIPS and IRS, further providing cross-calibration between all three instruments. IRAC's primary suite of standard calibration stars lies in the north ecliptic pole continuous viewing zone (Reach et al. 2005 PASP, 117, 978). Their stellar energy distributions were constructed by Cohen et al. (2003, AJ, 125, 2645) to tie directly to the absolute mid-infrared calibrations by Midcourse Space Experiment MSX (Price et al. 2004, SSRv 113, 409). Japan's AKARI mission uses the identical techniques and is tied to Spitzer by having absolute calibrators in common, drawn from the same networks (Ishihara et al. 2006, PASP, 118, 324). It was natural that WISE adopted the same approach to absolute and relative calibration so that data from all of these infrared missions can be simply co-analyzed.

The WISE team, in collaboration with the Spitzer Science Center, carried out a survey of the north and source ecliptic poles (NEP and SEP), the WISE "continuous viewing zones" (CVZs), using the full complement of Spitzer instrumentation: IRAC and MIPS broad-band mapping of a 47x47 arcmin (0.6 deg^2) region for each CVZ, and IRS spectroscopy of either previously identified calibrator stars or newly developed standard calibrators. The imaging and spectroscopic observations include the galaxy NGC 6552, which is used to cross-calibrate the long-wavelength band of WISE with the Spitzer IRS-LL and MIPS 24 micron channel.

The polar surveys were used to (i) provide consistent calibrators in both of the WISE CVZs, (ii) develop new calibrators near the south ecliptic pole where few existed previously , (iii) establish the photospheric character of all candidate calibrators, (iv) assess the long-term stability for secondary standards, (v) identify objects that would saturate the WISE arrays, (vi) identify galaxies that are resolved by IRAC, and measure their properties using methods appropriate to extended sources, and (vii) study the extragalactic population. The observations, results and analysis are presented in Jarrett et al. (2011).

Because of the scarcity of W4 calibrators near the ecliptic poles, a set of W4 calibrators located further from the poles are selected to supplement the initial set of W4 WISE calibrators. The complete set of WISE photometric calibrators is listed in Tables 7a-7d.

Tables 7a-7d - WISE Photometric Calibration Sources

iii. Calibrated Magnitudes

The instrumental source brightness measurements made by the pipeline photometry module (IV.4.c) are calibrated by adding an *instrumental zero point magnitude*. The calibrated magnitudes given in the WISE All-Sky Release Source Catalog and Single-exposure Source Database magnitudes are given by:

$$M_{cal} = M_{0,inst} - 2.5*log_{10}(flux) - [AC]$$

where

- M_{cal} is the calibrated magnitude
- $M_{0,inst}$ is the instrumental zero point (magnitudes); given in Table 8, below
- *flux* is the integrated, background subtracted source brightness, measured in in digital numbers (DN), or the 2-σ upper limit to the flux (see IV.4.c.iv.5)
- *AC* is the aperture correction, applied only for the standard aperture magnitudes, *w?mag*; given in Table 4 in IV.4.c.iv.2

The instrumental zero point magnitudes are band-dependent, and are different for the photometry in the All-Sky Release Catalog/Reject Table and Single-exposure Source Database. The zero point derivation is described in IV.4.h.iv.

iv. Photometric Zero Point Evaluation

The instrumental zero point magnitudes for photometry on the Single-exposure images were derived using the measurements of the calibration sources made during each scan. The zero point magnitudes, $M_{0,inst}$, were computed for each band, b, and are equal to the average difference between the prior, "true" magnitude of each calibrator and the instrumental magnitude measured by the Scan/frame Pipeline.

$$M_{0,inst,b} = AVG(M_{p,b} - M_{m,b})$$

where $M_{p,b}$ is the prior, "true" magnitude of the calibrator, and $M_{m,b}$ is the measured, instrumental magnitude in band, b. The instrumental zero points used for the Single-exposure Source Database for the full cryogenic survey phase are listed in Table 8. The RMS values listed are the root variance of the differences between the true and measured magnitudes for all calibration source measurements. The standard deviations of the mean instrumental zero points are <<1% for all bands because thousands of measurements are used to evaluate them. The Single-exposure database instrumental zero point magnitudes are also carried in the MAGZP values in the Single-exposure FITS headers and w?zero values in the Frame Metadata Table.

Initial estimates of the Single-exposure instrumental zero point values were made early in the WISE survey and were used to calibrate photometry during first-pass processing. The zero points were refined prior to second-pass processing and were based on analysis of all measurements of the calibration sources over the full cryogenic survey phase.

The instrumental zero point magnitudes used to calibrate source measurements in the Multiframe Pipeline for the All-Sky Release Source Catalog and Reject Table are *selected* values that are similar but not identical to the Single-exposure instrumental zero points. Pixel values in each of the Single-exposure images contributing to an Atlas Image were scaled to a common gain in the throughput matching step of the Atlas Image Generation module, using factors computed from the instrumental zero points of the individual exposures and the pre-defined Atlas Image zero point. This scaling step was designed to accomodate possible changes in the system throughput throughout the survey. No measurable throughput changes were seen during the full cryogenic survey phase, but significant changes were measured during the 3-Band Cryo and Post-Cryo phases. The Catalog and Reject Table instrumental zero point magnitudes listed in Table 8 are also carried in the MAGZP values in the Atlas Image FITS headers and w?magzp values in the Atlas Image Metadata Table.

Table 8 - Instrumental Zero Point Magnitudes for WISE All-Sky Release Source Photometry

Band	**wavelength (μm)**	**Single-exposure Source Database**		**Source Catalog and Reject Table**
		$M_{0,inst}$ (mag)	**RMS (mag)**	**$M_{0,inst}$ (mag)**
W1	**3.4**	20.752	0.032	20.5
W2	**4.6**	19.596	0.037	19.5
W3	**12**	17.800	0.051	18.0
W4	**22**	12.945	0.063	13.0

In Figures 3a through 3d are shown the differences between true and measured Single-exposure magnitudes that have been calibrated using the instrumental zero points in Table 8, for all calibrators, plotted as a function of time. For W4 in figure 3d, the blue and red points represent the residuals for stellar (blue) calibrators and the Seyfert galacy NGC6552 (red) calibrator, respectively. The discrepancy between the blue and red source measurements is discussed in IV.3.g.vii. These residual time histories illustrate that the WISE system photometric throughput was extremely stable over the period of the full cryogenic survey. The average residuals between true and measured magnitudes is 0.008, -0.001, -0.001 and 0.028 mag in the four bands, respectively.

The WISE photometric stability is even better than represented by Figures 3a-3d. Some of the apparent scatter in the time histories of the photometric residuals comes from uncertainty in the knowledge of the "true" brightness of the calibration sources. Figures 4a-4c show the time history of the W1-W3 zero point residuals, as in Figures 3a-3c, but in each of these plots residuals from a single calibrator are shown in green. The scatter in the single source distributions is noticeably smaller than for the ensemble, and the corresponding RMS values are commensurate: 0.023, 0.024 and 0.025 mag in W1, W2 and W3, respectively. Only one of the W4 calibration sources, NGC6552, is near an ecliptic pole and was therefore monitored continuously during the survey. The blue calibrators are all at lower ecliptic latitudes, and thus different calibrators are observed at different times. This combined with inherent uncertainties in their true 22µm fluxes produces the apparent large temporal variation in the residuals seen in Figure 3d.

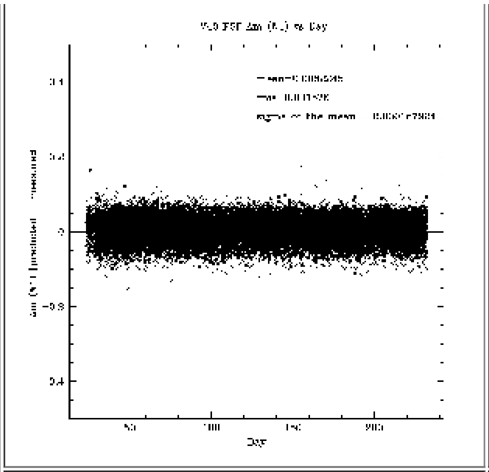

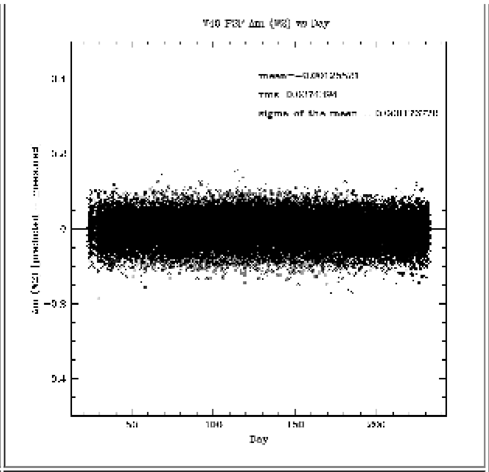

Figure 3a - W1

Figure 3b - W2

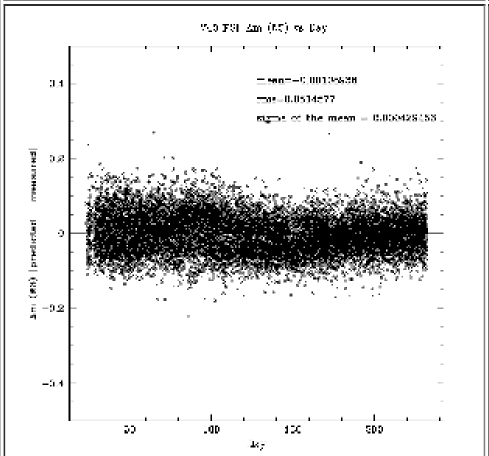

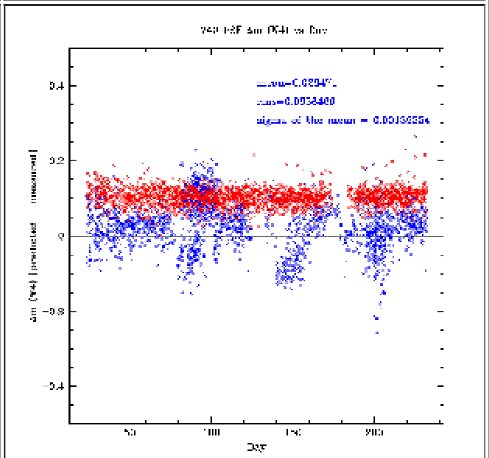

Figure 3c - W3

Figure 3d - W4

Differences between "true" (predicted) and measured Single-exposure magnitudes for all WISE primary calibration sources, plotted as a function of 2010 day number. The measured magnitudes were calibrated using the Single-exposure instrument zero points listed in Table 8. For W4, the residuals for stellar calibrators and NGC6552 are shown in blue and red, respectively.

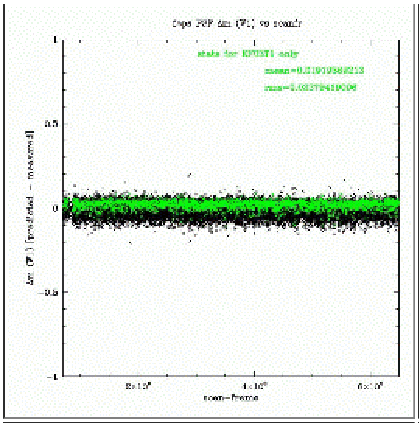	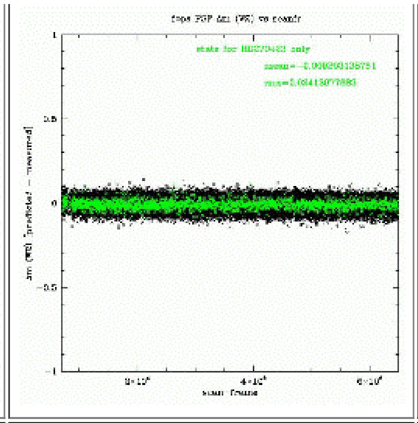	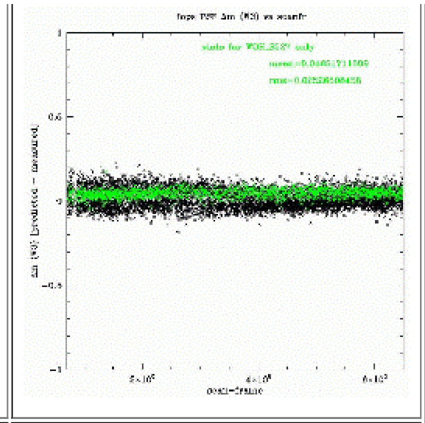
Figure 4a - As in Figure 3a, but with W1 Primary Calibrator: KF03T1 M_p=9.88 mag plotted in green (Detail)	**Figure 4b** - As in Figure 3b, but with W2 Primary Calibrator: HD270422 M_p=7.38 plotted in green (Detail)	**Figure 4c** - As in Figure 3c, but with W3 Primary Calibrator: WOH_S527 M_p=7.50 plotted in green (Detail)

v. WISE Filter Bandpasses and Zero Magnitude Attributes

The WISE relative system response curves (RSRs) were created from the end-to-end lab measurements by modifying the prediction and design values at each wavelength by fitting a line in log-log space and using this to replace any originally negative values. Following the prescription of Bessell (2000), we convert the QE-based Wright et al. (2010) RSRs (Fig. 5) from electrons per photon to photon-counting response curves by multiplying by λ and renormalizing each curve to a peak of unity; see Fig. 5b. Both W1 and W2 passbands have close correspondence with those of IRAC-1 and IRAC-2, although the W1 passband is slightly `blue' compared to IRAC-1 and W2 is slightly `red' compared to IRAC-2. The reddest channel of WISE, W4 at 22 μm, compares well with MIPS-24, although it is slightly bluer in response. Compared to Spitzer imaging, the only unique band of WISE is that of W3 (12 μm) which has only small overlap with that of IRAC-4 (8 μm), but is comparable to the IRAS 12 μm channel. One consequence of this band-to-band difference is demonstrated in Fig. 4b, the spectrum of ultra-luminous infrared galaxy Arp 220 has strong polycyclic aromatic hydrocarbon (PAH) emission bands, notably at 11.3 μm compared to the bands at 6.2 and 7.7 μm. WISE W3 compared to IRAC-4 will be more sensitive to both PAH emission and amorphous silicate absorption (10 μm) in nearby star-forming galaxies. Moreover, because W3 is a longer wavelength channel than IRAC-4, it is more sensitive to higher redshift galaxies in which strong near-IR continuum and mid-IR emission features redshift into the band.

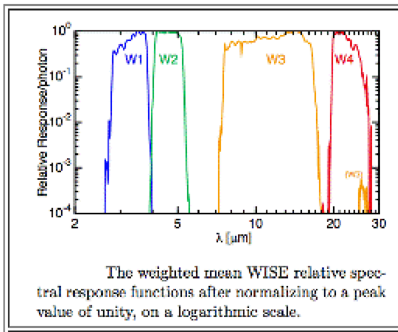	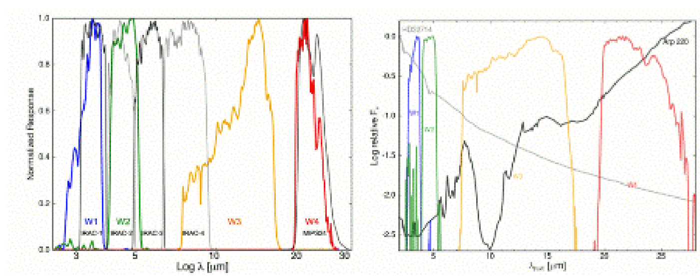
Figure 5a - The QE-based (response per photon) relative system response (RSR) curves normalized to a peak value of unity, on a logarithmic scale. The QE-based RSRs in ASCII table format are available for W1, W2, W3, and W4, which includes wavelength in microns, the response, and the uncertainty in the response in parts per thousand (from Wright et al. 2010).	**Figure 5b** - WISE energy based relative system response (RSR) curves, λR(λ), normalized to unity. (Left) The WISE RSRs of W1 (3.4μm; blue), W2 (4.6μm; green), W3 (12μm; orange), and W4 (22μm; red) are compared to the Spitzer IRAC-1 (3.6μm), IRAC-2 (4.5μm), IRAC-3 (5.8μm), IRAC-4 (8.0μm), andMIPS-24 (24μm) array-averaged response curves (all shown with black and gray lines). (Right) Contrasting spectra, the starburst galaxy Arp 220 (Armus et al. 2007 ApJ, 656, 148) and the K2III calibration star HD32174 spectra are shown in relation to the WISE RSRs. The response per unit energy RSRs in ASCII table format are available for W1, W2, W3, and W4, which include wavelength in microns, the response, and the uncertainty in the response in parts per thousand (from Jarrett et al. 2011).

Table 9 - WISE Zero Magnitude Attributes (from Jarrett et al. 2011)

WISE Zero Magnitude Attributes

Band	In-Band W cm^{-2} Unc(InBd) W cm^{-2}	Bw μm Unc(Bw) μm	F_λ(iso) W cm$^{-2}\mu$m^{-1} Unc(F_λ) W cm$^{-2}\mu$m^{-1}	λ(iso) μm Unc(λ) μm	Bw Hz Unc(Bw) Hz	ν(iso) Hz Unc(ν) Hz	F_ν(iso) Jy Unc(F_ν) Jy	F^*_ν(iso) Jy Unc(F_ν) Jy	AB mag
W1	5.4188E-15	6.6256E-01	8.1787E-15	3.3526	1.7506E+13	8.8560E+13	309.540	306.682	2.699
	7.9666E-17	1.2168E-03	1.2118E-16	0.0132	3.0407E+10	7.2306E+11	4.582	4.600	
W2	2.5172E-15	1.0423E+00	2.4150E-15	4.6028	1.4653E+13	6.4451E+13	171.787	170.663	3.339
	3.6858E-17	1.0982E-03	3.5454E-17	0.0168	1.1759E+10	5.0629E+11	2.516	2.600	
W3	3.5878E-16	5.5069E+00	6.5151E-17	11.5608	1.1327E+13	2.6753E+13	31.674	29.045	5.174
	5.3306E-18	1.6942E-02	9.8851E-19	0.0446	8.5791E+09	1.9731E+11	0.450	0.436	
W4	2.0876E-17	4.1013E+00	5.0901E-18	22.0883	2.4961E+12	1.3456E+13	8.363	8.284	6.620
	3.7888E-19	4.4812E-02	1.0783E-19	0.1184	4.0207E+09	1.0049E+11	0.124	0.124	

Note. — The 'idealized' Vega in-band flux is measured by spectrally integrating over the peak-normalized WISE photon-counting RSRs (see Fig. 1). Dividing by the RSR bandwidth, Bw(λ), the resultant passband mean flux density, F_λ(Vega), represents the λ(iso) monochromatic or isophotal flux density, F_λ(iso). Likewise, F_ν(iso) is the constant F_ν that gives the same response as Vega: F_ν(Vega) = F_ν(iso); it is derived from the WISE photon-counting RSRs cast in frequency terms. It can also be computed as F^*_ν(iso)/f_0 where F^*_ν(iso) and the flux correction factor, f_0, are given in Wright et al. (2010). For example, for a source with spectrum F_ν=constant, the correction factors are 0.991, 0.994, 0.917 and 0.991, for W1, W2, W3 and W4, respectively. The monochromatic AB magnitudes are computed from -2.5×log10[F_ν(iso)] + 8.926 (Tokunaga & Vacca 2005).

Adopting a stellar photospheric spectrum, specifically that for an "ideal" Vega in which the effective temperature is uniform across the stellar surface (described in Cohen et al. 1992), the system, or isophotal wavelengths, λ(iso), are found to be 3.35, 4.60, 11.56, and 22.08 μm (see also Wright et al. 2010). The isophotal flux $F_{\lambda(iso)}$ was derived by integrating the modified Vega spectrum across the WISE RSRs. For the frequency equivalent integral, F_ν(iso), we applied the method described in Cohen et al. (1999) and Tokunaga & Vacca (2005), recasting each WISE RSR in frequency terms and integrating the stellar spectrum over the RSR to derive the in-band flux. The resultant isophotal quantities and other WISE system attributes are given in Table 8 for both wavelength-based and frequency-based RSRs. Note that Wright et al. (2010) use a different treatment to calculate the F_ν(iso) values that is based on the direct conversion of λ(iso) to F_ν using the formulation F_ν(iso) equals (λ^2(iso)/c)$F_{\lambda(iso)}$; this method is strictly an approximation used for narrow-band filters and is typically unsuitable for wide passbands (Cohen et al. 1999, their Sec. 3.3; and the standard method is restated by Tokunaga & Vacca 2005). The approximation is in fact adequate for W1, W2 and W4. Wright et al. (2010) provide a set of flux corrections, f_c, that properly transform from F_ν^*(iso) to `in-band' F_ν(iso): $F_{\nu 0} = F^*_{\nu 0} / f_c$, notably important for W3 and its broad passband.

Absolute measurements of stars and comparisons of stellar irradiances with those of emissive reference spheres were made by MSX. This `ideal' Vega spectrum was absolutely validated by photometry on the MSX and provided the basis for defining the zero magnitude for Infrared Space Observatory (ISO), MSX, Spitzer, and AKARI infrared space telescopes. This validated zero magnitude system is traceable to measurements using K (primary) and M giant (secondary) calibrators and has an absolute precision of ±1.10%. This basis now serves the same purpose for the four WISE bands, ensuring that their photometric calibrations have been computed in the same manner as for these previous missions.

The in-band fluxes of the Vega spectrum were adopted to define zero magnitude for WISE bands W1, W2, and W3. Data for W4 incorporate the 2.7% upward offset from the Vega basis model that was established absolutely by MSX at 21.3 μm (Price et al. 2004: Table 4, Column 7, and Table 9, Column 2), and applied by Cohen (2009) in the validation of the diffuse calibration of Spitzer MIPS-24 by comparison with the MSX 21.3 μm band. This Vega basis has an overall systematic uncertainty of ~1.45%.

vi. Flux Corrections and Colors for Power Laws and Blackbodies

Wright et al. (2010) define the photometric system for WISE as follows:

> This definition of the isophotal wavelength and flux zeropoint means that the color correction term for a source with a different spectrum than Vega vanishes by construction when f_λ is a constant ($f_\nu \sim \nu^{-2}$) and very nearly vanishes for Rayleigh-Jeans sources with $f_\lambda \sim \lambda^{-4}$ or $f_\nu \sim \nu^2$. These spectral energy distributions bracket those of the vast majority of WISE sources, so the color corrections are generally small. But the extremely wide W3 filter does lead to color corrections as large as 0.1 mag for a constant f_ν. Table 10 (identical to Table 2) gives the flux correction factors in the WISE bands for several input spectra and the WISE colors for these spectra. These factors multiply the signal S given by a spectrum $f_\nu = f_\nu^o(\lambda(iso) / \lambda)^\beta$. Thus, a spectrum with f_ν = const = 29.0 Jy gives a signal that is f_c(W3) = 0.9169 times the signal from Vega, so one would need a constant f_ν of 29.0/0.9169 = 31.7 Jy to give zero magnitude.

Table 10 - Color corrections (from Wright et al. 2010)

FLUX CORRECTIONS AND COLORS FOR POWERLAWS AND BLACKBODIES

F_ν	$f_c(W1)$	$f_c(W2)$	$f_c(W3)$	$f_c(W4)$	[W1-W2]	[W2-W3]	[W3-W4]
ν^3	1.0283	1.0206	1.1344	1.0142	-0.4040	-0.9624	-0.8684
ν^2	1.0084	1.0066	1.0088	1.0013	-0.0538	-0.0748	-0.0519
ν^1	0.9961	0.9976	0.9393	0.9934	0.2939	0.8575	0.7200
ν^0	0.9907	0.9935	0.9169	0.9905	0.6393	1.8357	1.4458
ν^{-1}	0.9921	0.9943	0.9373	0.9926	0.9828	2.8586	2.1272
ν^{-2}	1.0000	1.0000	1.0000	1.0000	1.3246	3.9225	2.7680
ν^{-3}	1.0142	1.0107	1.1081	1.0130	1.6649	5.0223	3.3734
ν^{-4}	1.0347	1.0265	1.2687	1.0319	2.0041	6.1524	3.9495
$B_\nu(100)$	17.2062	3.9096	2.6588	1.0032	10.6511	18.9307	4.6367
$B_\nu(141)$	4.0882	1.9739	1.4002	0.9852	7.7894	13.0371	3.4496
$B_\nu(200)$	2.0577	1.3448	1.0006	0.9833	5.4702	8.8172	2.4949
$B_\nu(283)$	1.3917	1.1124	0.8791	0.9865	3.8329	5.8986	1.7552
$B_\nu(400)$	1.1316	1.0229	0.8622	0.9903	2.6588	3.8930	1.2014
$B_\nu(566)$	1.0263	0.9919	0.8833	0.9935	1.8069	2.5293	0.8041
$B_\nu(800)$	0.9884	0.9853	0.9125	0.9958	1.1996	1.6282	0.5311
$B_\nu(1131)$	0.9801	0.9877	0.9386	0.9975	0.7774	1.0421	0.3463
K2V	1.0038	1.0512	1.0030	1.0013	-0.0963	0.1225	-0.0201
G2V	1.0049	1.0193	1.0024	1.0012	-0.0268	0.0397	-0.0217

vii. Calibration Uncertainties

Photometric performance is gauged using the individual and time history measurements of the WISE calibrators. The RMS residuals in the zero point offset for each WISE band (Table 8) provide a measure of the accuracy of the calibration solution, while the time history provides a metric for the photometric stability over the lifetime of the cryogenic mission (Figure 3).

Figure 6 shows the time history of the difference between the predicted (true) and measured magnitudes for the ensemble of calibration stars, average in coarse time bins. In Figure 7 are shown the mean and standard deviation of the flux residuals for each calibration source, plotted as a function of the source brightness.

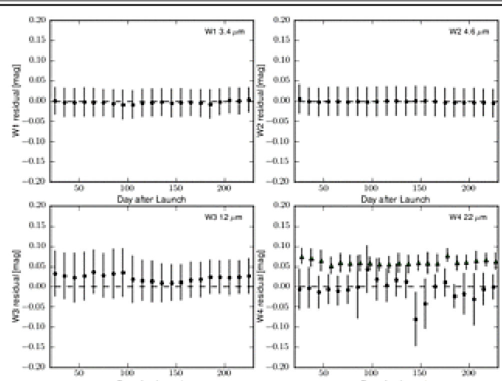

WISE instrumental zero point magnitude time history. The binned average residual flux for the ensemble of calibration stars is plotted over the lifetime of the cryogenic mission, where the residual flux is the difference between the calibration (predicted) value and the WISE measurement. The ensemble mean and standard deviation of the mean are: -0.003 ± 0.001, -0.001 ± 0.001, 0.022 ± 0.002, -0.007 ± 0.005, for W1, W2, W3 and W4, respectively. NGC 6552, denoted with a triangle for the W4 measurements, is offset from the mean by 6.1% with a small scatter of 0.1% about its mean. See Fig. 8 for the individual calibrator results.

Figure 6 - WISE instrumental zero point magnitude time history (from Jarrett et al. 2011).

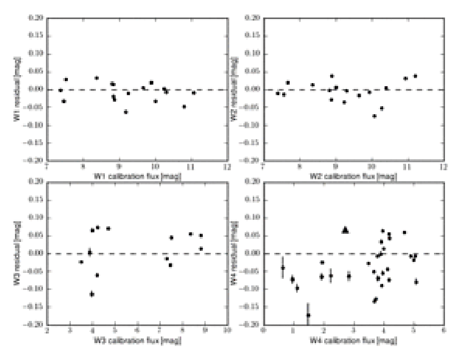

WISE photometry of the *Spitzer*-WISE cross-calibration stars. The residual flux is the difference between the calibration (predicted) value and the WISE measurement (with error bars). The RMS scatter is 2.4, 2.8, 4.5 & 5.7% for W1, W2, W3 and W4, respectively. NGC 6552 is denoted with a triangle for the W4 measurements.

Figure 7 - WISE photometry of the Spitzer-WISE cross-calibration stars (from Jarrett et al. 2011).

Time variability in the instrumental zero point magnitude is ruled out with individual (repeated) measurements over the lifetime of the mission; repeated observations of the individual calibrators reveal an RMS scatter, typically better than 1% (Figure 6). In contrast, the ensemble plotted in Figure 7 has a much larger scatter than the trending in the zero point. For both W1 and W2, the inverse variance-weighted mean is 0.007 +- 0.025 mag, for W3 it is 0.017 &plusm; 0.045 mag, and for W4, it is -0.021 &plusm; 0.057 mag. The ensemble results suggest that the WISE absolute calibration, tied to that of Spitzer, has an RMS scatter in the standard calibration stars at the 2.4, 2.8, 4.5 & 5.7% levels for W1, W2, W3 and W4, respectively.

The observed scatter in Figure 7 arises chiefly from the uncertainty in the predicted WISE flux values for the calibration sources, reflecting the inherent errors associated with model fitting to the broad-band SED measurements, as well as the uncertainty in the WISE RSRs. These errors are much larger then the expectation at the longer mid-IR wavelengths, notably in the W4 window -- the red calibrator NGC 6552 has a W4 residual of ~6%, a difference that appears to be systematic for very red sources as measured using Spitzer-IRS spectra from ultra-luminous infrared galaxies (see Wright et al. 2010).

Discrepancy between blue and red source measurements

Photometric calibration is based on measurements of bright stars, A-K dwarfs and K/M giants, which are relatively blue in color in comparison to star-forming galaxies, for example. As shown in Figures 3d above, the Sy-2 galaxy NGC 6552 appears to have a significantly different zero point offset compared to the bluer stellar calibrators. This difference has been observed in other red extragalactic objects, notably ultra-luminous infrared galaxys (ULIRGs). Wright et al. (2010) describe the blue vs. red calibration discrepancy as follows:

> We have also observed in-flight a discrepancy between red (typically sources with $f_\nu \sim \nu^{-2}$) and blue (stars with $f_\nu \sim \nu^2$) calibrators in W3 and W4, the 12 and 22μm bands. This amounts to about -17% and 9% in the fluxes for W3 and W4, with the red sources appearing too bright in W4 and too faint in W3. The flux differences could be resolved by adjusting the effective wavelength of W3 and W4 3%-5% blueward and 2%-3% redward, respectively. This would change the zero magnitude f_ν^o by about -8% in W3 and +4% in W4. But the zeropoints and isophotal wavelengths reported here are based on the relative spectral responses derived from ground calibration without any such adjustment. The instrumental zeropoints that define the conversion from counts to magnitudes have been based on standard stars, which are the blue calibrators. Given the discrepancy between red and blue calibrators we estimate that the conversion from magnitudes to Janskys are currently uncertain by 10% in W3 and W4.

Last update: 2012 August 20

Previous Contents Next